## Raman spectroscopy and NIR as a method of comparing monofloral and honeydew honeys

Boris Pleva<sup>1</sup>, Matej Pospiech<sup>1</sup>, Alena Saláková<sup>2</sup>, Martina Pečová<sup>1</sup>, Jana Čaloudová<sup>1</sup>, Zdeňka Javůrková<sup>1</sup>, Pavel Hrabec<sup>3</sup>, Bohuslava Tremlová<sup>1</sup>

<sup>1</sup>University of Veterinary Sciences Brno, Faculty of Veterinary Hygiene and Ecology,
Department of Plant Origin Food Sciences, Brno, Czech Republic

<sup>2</sup>Mendel University in Brno, Faculty of AgriSciences, Department of Food Technology, Brno, Czech Republic

<sup>3</sup>University of Technology Brno, Faculty of Mechanical Engineering,
Department of Computer Graphics and Geometry, Brno, Czech Republic

Received June 26, 2025 Accepted September 10, 2025

#### Abstract

Honey is one of the most commonly adulterated foods. This study therefore focused on innovative possibilities of identifying the botanical origin of honey using Raman spectroscopy and Fourier transform near-infrared spectroscopy (FT-NIR), in order to test their potential use as an alternative to physicochemical analysis and melissopalynology methods. Both mentioned non-destructive methods were used for discrimination and characterization of the honey species. Forty-seven samples of flower and honeydew honey obtained from hobby beekeepers from different regions of the Czech Republic were analysed in the period between 2019 and 2021. Among the floral honeys, poly- as well as monofloral honeys were selected (rapeseed, clover, acacia, phacelia, fruit tree honey). The FT-NIR analysis results confirmed significant differences (P < 0.05) between the specific-species honey samples for wavenumbers of 5,624, 5,171, 4,780,  $4,391 \text{ cm}^{-1}$  (P < 0.05). Raman spectroscopy confirmed significant differences between multiple wavenumbers, with classification into the most classes confirmed for wavenumbers of 308, 606, 613, 620, 999 and 1,013 cm<sup>-1</sup> (P < 0.05). However, neither method allowed classification for all honey species, thus FT-NIR and Raman spectra were compared by linear discriminant analysis (LDA), which confirmed a high correct classification rate (CCR) of 99.38%, and 91.30% in the case of cross-validation. In the case of rapeseed honey, the lowest CCR (96.15%) and cross-validation (76.92%) values were confirmed. It was confirmed that the FT-NIR method in combination with Raman spectroscopy can be used to identify individual honey species with a high degree of reliability.

Foodstuff adulteration, non-destructive analysis, wavenumber

Honey is a natural product of the honey bee and is produced by converting the nectar of flowering plants or by the activity of aphids through the filtration of tree sap. The characteristic sensory properties of honey, such as aroma, flavour, colour and composition, are mainly influenced by its botanical and geographical origin, which is closely related to the seasonality of each plant species (Mandal and Mandal 2011; Samarghandian et al. 2017). The properties and composition of honey depend to a large extent on the species of flowers of the plants, or on the type of honeydew the bees collect. These differences play an important role in the sensory properties and its chemical composition. The composition of honey also influences the subsequent extraction, processing, and storage. Honey is a complex food composed of more than 200 compounds, 80% of which are carbohydrates, of which the monosaccharides glucose and fructose are the most abundant, 17% is water and the remaining 3% are other components (Bogdanov et al. 2008; Combarros-Fuertes et al. 2020). It also contains bioactive compounds that exhibit antimicrobial properties, which are also attributed to the high osmotic pressure, low water content, and pH. Other compounds showing antimicrobial effects include hydrogen peroxide,

Matej Pospiech Department of Plant Origin Food Sciences Faculty of Veterinary Hygiene and Ecology University of Veterinary Sciences Brno Palackého tř. 1946/1, 612 42 Brno, Czech Republic methylglyoxal, bee defensin, polyphenols and volatile compounds (Jerković and Kuś 2014; Samarghandian et al. 2017). Honey also exhibits antioxidant effects, which are associated with the presence of polyphenolic compounds, mainly phenols and flavonoids, their acids and derivatives, enzymes such as catalase and peroxidase, as well as proteins, amino acids and other compounds (Ahmed et al. 2018; Cianciosi et al. 2018).

Recently, there has been a growing interest in single-species flower honeys, which are characterised not only by their specific sensory properties but also by their medicinal effects, which vary according to their botanical origin. This has resulted in their frequent adulteration, especially by mislabelling plant species (El Sohaimy et al. 2015; Tsagkaris et al. 2021). Honey adulteration is a significant issue driven by economic motivations. While the historical documentation of honey adulteration is extensive, it remains prevalent today due to outdated standards, inappropriate analytical methods, and inefficient traceability and auditing systems (García and Amadei Enghelmayer 2025).

Raman spectroscopy and Fourier transform near-infrared spectroscopy (FT-NIR) were selected as alternative methods for the detection of possible adulteration of honey. The aim of this study was to determine whether these methods are suitable and comparable to traditional analytical methods or as complementary methods, as well as whether differences between the individual honey types can be detected, thus confirming the suitability of both methods.

### Material and Methods

## Sample preparation

Honey from hobby beekeepers from all over the Czech Republic was used for the analysis. A total of 47 honey samples were analysed, of which 5 were honeydew (Hd), 27 were polyfloral (Pf), 8 were rapeseed (Bn), 2 were acacia (Rp), 2 were fruit tree (Pp), 1 was phacelia (Pt) and 2 were clover (Tr). For Raman spectroscopy and FT-NIR examination, 10 g of honey sample was standardized by dilution with distilled water to 65° Brix

Table 1. Description of individual vibrations at wavenumbers ranging from 300 to 7,000.

Wavenumber	Vibration
(cm <sup>-1</sup> )	
6,854	C-H, O-H, N-H energy corresponds to the second overtone or combination bands (Smith 2011)
5,624	O-H and C-H stretching regions of the saccharides (Rodriguez-Saona et al. 2001)
5,171	C-O and C-C stretching regions of the saccharides (Ruoff et al. 2006)
4,780	C-O and C-C stretching regions of the saccharides (Ruoff et al. 2006)
4,391	C-O and C-C stretching regions of the saccharides (Ruoff et al. 2006)
1,226	deformation vibration of C-C-H, O-C-H, and C-O-H (Pierna et al. 2011)
1,135 ~	C-O-H group deformation vibration (Pierna et al. 2011)
1,094 ~	(C-O-C) angle-bending (Ozbalci et al. 2013)
	(C-O) vibration in the pyranoid and furanoid rings
1,027 ~	C-O) vibration in the pyranoid and furanoid rings (Ozbalci et al. 2013)
991 ~	deformation of C-H out of the pyranoid (Mathlouthi and Luu 1980)
926	deformation of C- H out of the furanoid ring (Mathlouthi and Luu 1980)
844	(C-C) and (C1-H1) vibrations (Ozbalci et al. 2013)
829 ~	C-H and CH2 vibrations and C-O-H bending (Aykas et al. 2020)
695	stretching of C-O and C-C-O, O-C-O bending (Anjos et al. 2018)
615 ~	ring deformations (Anjos et al. 2018)
553 ~	α-glycosidic bond of C1 on the glucosyl subunit (Ozbalci et al. 2013)
349	(C-C-C) ring vibration of pyranoid and furanoid forms (Ozbalci et al. 2013)
329	skeletal vibrational modes of C-C-C, C-C-O, C-O and C-C bonds (Wu 2022)
308	(C-C-C) vibration and an endocyclic (C-C-O) ring deformation (Ozbalci et al. 2013)

Significant difference between monofloral honey and honeydew honey, significance level P < 0.05,  $\sim$  average value

using a PAL benchtop refractometer (Atago, Tokyo Japan). This standardization step was performed to reduce fluorescence (Magdas and Berghian-Grosan 2023). The diluted honey sample was dissolved in an ultrasonic bath (Bandelin, Berlin, Germany) and after tempering to room temperature, the desired refraction was rechecked.

## Honey determination by Raman

Honey samples were analysed in 4 ml cuvettes using Raman spectroscope WP RAMAN 785 (Wasatch Photonics, Morrisville, NC, USA) in the range of 300–2,000 wavenumber cm<sup>-1</sup> using a laser, 785 nm narrow linewidth diode laser, stabilized using volume holographic grating technology, (Ondax, Monrovia, CA, USA) with a wavelength of 785 nm and a power of 91 mW. Each sample was prepared in duplicate and each of these duplicates was measured twice. For each measurement, the device averaged 8 consecutive measurements of the same sample. A total of 32 spectral scans were measured (Table 1).

## Honey determination by FT-NIR

The samples were measured in 30 mm cuvettes in triplicate. Reflectance of the rays was enhanced using a 0.2 mm metallic mirror. NIR spectra were acquired using an Antaris II (Thermo Scientific, Waltham, MA, USA) equipped with a tungsten-halogen source, an integrating sphere, and an InGaAs detector. The signal was collected in transflectance mode using the integrating sphere, with the cuvette positioned on the optical window. Spectra were recorded at room temperature in the 10,000–4,000 cm<sup>-1</sup> range, accumulating 64 scans at a nominal resolution of 8 cm<sup>-1</sup>. After subtracting the blank spectrum, the spectra were converted to pseudo-absorbance (A = log(1/R); R = reflectance). The spectroscopic data acquisition was performed using the TQ Analyst software (Thermo Scientific) (Table 2).

## Statistical analysis

The data were statistically evaluated using XLSTAT 2024.2.0 (Lumivero, Denver, CO, USA). Normality of the data was confirmed with Shapiro-Wilk test. For the maximum intensity of important peaks, ANOVA with post hoc Duncan's test was applied. Linear discriminant analysis was performed with the following parameters: a significance level of 5%, a forward selection model, and an input threshold value of 0.05.

## Results

Factor analysis was employed to evaluate the individual wavenumbers of the Raman spectra and FT-NIR spectra, as well as their mutual correlation. The results are presented in Fig. 1 (Plate X and Table 2). The eigenvalues obtained were 31.51, 59.25, 81.52, 90.59, 96.91, and 100, corresponding respectively to the factors F1, F2, F3, F4, F5, and F6.

The honey samples were analysed by Raman spectroscopy, which revealed significant peaks at the following wavenumbers: 308, 329, 349, 553, 615, 695, 829, 844, 926, 991, 1,027, 1,094, 1,135, and 1,226 cm<sup>-1</sup> (Table 3). These peaks are shown in Fig. 2 (Plate X). These specific wave numbers can be attributed mainly to the vibrations of the major constituents, especially carbohydrates. However, they can also be associated with other components, such as proteins, minerals, pollen grains and other components present in honey.

Table 2. Comparison of FT-NIR	(4,000–7,000 cm <sup>-1</sup> ) fo	r different honey types.

Sample/					
Wavenumber	6,854	5,624	5,171	4,780	4,391
(cm <sup>-1</sup> )					
Bn	$6,\!850.86 \pm 3.30^{a^*}$	$5,625.21 \pm 2.74$ ab	$5,165.14 \pm 1.15$ b	$4{,}779.33 \pm 1.26^{c}$	$4,\!390.47 \pm 0.23^{a}$
Hd	$6,853.82 \pm 5.83$ a	$5,\!623.84 \pm 1.39^{ab}$	$5{,}167.12 \pm 2.97^{a}$	$4{,}783.29 \pm 3.08^{ab}$	$4{,}388.68 \pm 0.35^{\:b}$
Pf	$6,\!852.39 \pm 4.20^{a}$	$5,625.93 \pm 3.41$ a	$5{,}165.66 \pm 2.02^{b}$	$4{,}780.45 \pm 2.60^{c}$	$4,\!390.21\pm0.57^{\rm a}$
Pp	$6,854.23 \pm 5.49$ a	$5,621.96 \pm 3.35$ b	$5{,}168.83 \pm 3.63^{a}$	$4{,}784.34 \pm 3.11^{\rm \ a}$	$4,389.15 \pm 0.77^{c}$
Pt	$6,\!852.83 \pm 0.46^{a}$	$5,\!623.68 \pm 0.34^{ab}$	$5{,}164.92 \pm 0.09^{b}$	$4{,}779.07 \pm 0.06^{c}$	$4{,}390.18 \pm 0.18^{a}$
Rp	$6,\!853.27 \pm 0.17^{\rm a}$	$5,\!624.3\pm4.46^{ab}$	$5{,}164.93 \pm 0.09^{b}$	$4{,}781.56 \pm 3.39^{\mathrm{bc}}$	$4{,}389.65 \pm 0.59^{b}$
Tr	$6,\!853.55 \pm 0.90^{a}$	$5,\!624.44\pm2.64^{ab}$	$5{,}165 \pm 0.11$ b	$4{,}780.82 \pm 3.06^{\mathrm{bc}}$	$4,\!390.29 \pm 0.13$

a\*Mean  $\pm$  SD; Honey types: honeydew (Hd), polyfloral (Pf), rapeseed (Bn), acacia (Rp), fruit trees (Pp), phacelia (Pt), clover (Tr), different letter mean significant differences (P < 0.05) between the columns.

Table 3. Comparison of Raman wavenumber ranges (300-2,000 cm<sup>-1</sup>) across different honey types.

Vibrations (cm <sup>-1</sup> )	Bn	Hd	Pf	Pp	Pt	Rp	Ţ
308	$14,061.01 \pm 0.43$ d	$18,280.15 \pm 0.51$ abc	$16,365.79 \pm 0.23$ bed	21,237.68 ± 0.91 a	$18,907.12 \pm 1.01$ ab	$15,413.28 \pm 0.75 \mathrm{cd}$	$18,446.27 \pm 0.75$ abc
329	$9,387.14 \pm 0.43$ °	$12,164.49 \pm 0.51$ ab	$11,098.20 \pm 0.23$ b	$12,473.77 \pm 0.91$ <sup>a</sup>	$12,402.38 \pm 1.01$ ab	$10,469.35 \pm 0.75 \mathrm{cd}$	$13,911.92 \pm 0.75  \mathrm{abc}$
349	$8,133.34 \pm 0.43^{\text{ b}}$	$9,367.73 \pm 0.51$ <sup>b</sup>	$9,229.39 \pm 0.23$ b	$9,451.30 \pm 0.91$ b	$10,566.39 \pm 1.01$ ab	$8,851.65 \pm 0.75^{\mathrm{b}}$	$12,380.19 \pm 0.75$ <sup>a</sup>
543	$2,047.85 \pm 0.43$ <sup>a</sup>	$2,139.66 \pm 0.51$ <sup>a</sup>	$1,911.76 \pm 0.23$ <sup>a</sup>	$2,022.80 \pm 0.91$ ab	$1,324.09 \pm 1.01^{\circ}$	$1,352.58 \pm 0.75  \mathrm{bc}$	$1,102.2 \pm 0.75  \mathrm{bc}$
562	$2,359.91 \pm 0.43$ ab	$2,707.66 \pm 0.51$ <sup>a</sup>	$2,287.88 \pm 0.23$ ab	$2,574.55 \pm 0.91$ <sup>a</sup>	$1,914.9 \pm 1.01  \mathrm{bc}$	$1,927.17 \pm 0.75$ bc	$1,671.24 \pm 0.75^{\circ}$
602	$1,262.17 \pm 0.43$ <sup>a</sup>	$1,375.77 \pm 0.51$ <sup>a</sup>	$1,150.87 \pm 0.23^{\mathrm{b}}$	$1,223.52 \pm 0.91$ ab	$1,014.82 \pm 1.01^{\mathrm{bc}}$	$1,024.34 \pm 0.75 \mathrm{bc}$	$933.62 \pm 0.75$ °
909	$1,146.44 \pm 0.43 \mathrm{bc}$	$1,328.21 \pm 0.51$ <sup>a</sup>	$1,081.26 \pm 0.23  \mathrm{bc}$	$1,261.30 \pm 0.91$ ab	$997.95\pm1.01\mathrm{bod}$	$983.20 \pm 0.75  \mathrm{cd}$	$859.84 \pm 0.75$ d
613	$436.77 \pm 0.43$ bc	$616.59 \pm 0.51$ <sup>a</sup>	$426.17 \pm 0.23$ °	$570.27 \pm 0.91$ ab	$359.87 \pm 1.01\mathrm{cd}$	$350.75 \pm 0.75  \mathrm{cd}$	$228.43 \pm 0.75^{d}$
614	$363.04 \pm 0.43^{\text{ b}}$	$537.29 \pm 0.51$ <sup>a</sup>	$349.75 \pm 0.23^{\mathrm{b}}$	$511.06 \pm 0.91$ a	$279.04 \pm 1.01$ bc	$276.33 \pm 0.75 \mathrm{bc}$	$162.42 \pm 0.75^{\circ}$
620	$105.71 \pm 0.43$ bc	$177.02 \pm 0.51$ <sup>a</sup>	$88.58 \pm 0.23 \mathrm{bc}$	$152.97 \pm 0.91$ ab	$30.96\pm1.01^{\mathrm{cd}}$	$63.34 \pm 0.75$ bed	$3.4 \pm 0.75  ^{ m d}$
621	$87.61 \pm 0.43$ b	$135.59 \pm 0.51$ <sup>a</sup>	$69.18 \pm 0.23^{\mathrm{b}}$	$111.71 \pm 0.91$ ab	$21.28 \pm 1.01$ bc	$49.74 \pm 0.75 \mathrm{bc}$	$2.02 \pm 0.75$ °
969	$1,538.86 \pm 0.43$ a	$1,402.22 \pm 0.51$ ab	$1,366.69 \pm 0.23$ ab	$1,098.86 \pm 0.91$ b	$1,271.29 \pm 1.01$ ab	$1,142.51 \pm 0.75$ ab	$1,293.68 \pm 0.75$ ab
828	$102.9 \pm 0.43$ a	$108.46 \pm 0.51$ <sup>a</sup>	$77.15 \pm 0.23$ b	$94.42 \pm 0.91$ ab	$82.85 \pm 1.01$ ab	$74.38 \pm 0.75^{\mathrm{b}}$	$74.4 \pm 0.75^{\mathrm{b}}$
829	$113.73 \pm 0.43$ ab	$124.76 \pm 0.51$ <sup>a</sup>	$84.11 \pm 0.23$ °	$110.27 \pm 0.91$ abc	$94.43 \pm 1.01$ abc	$86.66 \pm 0.75 \mathrm{bc}$	$80.13 \pm 0.75$ °
844	$242.94 \pm 0.43^{\text{ b}}$	$294.55 \pm 0.51$ <sup>a</sup>	$210.27 \pm 0.23$ °	$263.3 \pm 0.91 \mathrm{bc}$	$231.52 \pm 1.01$ bc	$229.20 \pm 0.75 \mathrm{bc}$	$210.98 \pm 0.75  \mathrm{bc}$
926	$123.37 \pm 0.43$ <sup>a</sup>	$85.21\pm0.51\mathrm{bc}$	$114.08 \pm 0.23$ a	$51.03 \pm 0.91$ °	$109.24 \pm 1.01$ ab	$104.79 \pm 0.75$ ab	$119.22 \pm 0.75  \mathrm{a}$
975	$4.75 \pm 0.43$ b	$1.98 \pm 0.51$ b	$3.96 \pm 0.23$ b	$16.06 \pm 0.91$ a	$0.56 \pm 1.01^{\mathrm{b}}$	$0.31 \pm 0.75^{\mathrm{b}}$	$0 \pm 0$
926	$4.87 \pm 0.43$ b	$2.55 \pm 0.51$ b	$3.47 \pm 0.23$ b	$22.52 \pm 0.91$ a	$0.56 \pm 1.01^{\mathrm{b}}$	$0.17 \pm 0.75^{\mathrm{b}}$	$0 \pm 0$
284	$20.28 \pm 0.43$ °	$35.04\pm0.51\mathrm{bc}$	$29.31\pm0.23\mathrm{bc}$	$28.46\pm0.91\mathrm{bc}$	$56.16 \pm 1.01^{\mathrm{b}}$	$20.2 \pm 0.75$ °	$184.04 \pm 0.75$ <sup>a</sup>
066	$35.85 \pm 0.43$ °	$82.67 \pm 0.51$ <sup>b</sup>	$52.81 \pm 0.23$ °	$63.95\pm0.91\mathrm{bc}$	$129.21 \pm 1.01^{\mathrm{b}}$	$3,814 \pm 0.75$ °	$324.68 \pm 0.75$ <sup>a</sup>
962	$35.02 \pm 0.43$ °	$88.14 \pm 0.51 ^\circ$	$56.2 \pm 0.23^{\circ}$	$33.98\pm0.91^\circ$	$170.22 \pm 1.01^{b}$	$35.26 \pm 0.75 ^{\circ}$	$344.12 \pm 0.75$ <sup>a</sup>
266	$41.49 \pm 0.43^{\circ}$	$82.36 \pm 0.51$ °	$56.88 \pm 0.23^{\circ}$	$50.6\pm0.91^\circ$	$149.14 \pm 1.01^{\mathrm{b}}$	$36.83 \pm 0.75 ^{\circ}$	$276.28 \pm 0.75$ <sup>a</sup>
666	$44.05 \pm 0.43$ b	$70.52 \pm 0.51$ °	$55\pm0.23^{\rm b}$	$55.04 \pm 0.91  ^{\mathrm{cb}}$	$113.04 \pm 1.01^{b}$	$40.12 \pm 0.75 \mathrm{d}$	$195.77 \pm 0.75$ <sup>a</sup>
1001	$41.54 \pm 0.43$ °	$54.4\pm0.51\mathrm{bc}$	$49.95\pm0.23\mathrm{bc}$	$54.66\pm0.91\mathrm{bc}$	$73.64 \pm 1.01^{\mathrm{b}}$	$37.14 \pm 0.75$ °	$121.9 \pm 0.75  \mathrm{a}$
1002	$45.29 \pm 0.43$ b	$54.23 \pm 0.51^{\mathrm{b}}$	$51.56 \pm 0.23$ b	$60.91 \pm 0.91$ b	$58.62 \pm 1.01^{\mathrm{b}}$	$40.83 \pm 0.75$ b	$92.5 \pm 0.75  \mathrm{a}$
1026	$70.02 \pm 0.43$ b	$69.74 \pm 0.51^{\mathrm{b}}$	$67.21 \pm 0.23$ b	$93.47 \pm 0.91$ a	$41.51 \pm 1.01^{\circ}$	$61.35 \pm 0.75 \mathrm{bc}$	$43.47 \pm 0.75$ °
1028	$60.19 \pm 0.43$ b	$57.89 \pm 0.51$ <sup>b</sup>	$59.39 \pm 0.23$ b	$92.22 \pm 0.91$ a	$32.07 \pm 1.01^{\circ}$	$57.67 \pm 0.75$ b	$38.02 \pm 0.75$ °
1056	$30.51 \pm 0.43$ a	$12.4\pm0.51^{\rm bc}$	$22.66\pm0.23\mathrm{ab}$	$6.51 \pm 0.91^{\circ}$	$11.07\pm1.01\mathrm{bc}$	$19.93 \pm 0.75$ ab	$13.17\pm0.75\mathrm{bc}$
1111	$14.1 \pm 0.43  ^{\mathrm{a}}$	$3.14 \pm 0.51^{\mathrm{b}}$	$5.8 \pm 0.23$ b	$7.22 \pm 0.91$ b	$0 \pm 0$	$1.24 \pm 0.75$ b	$1.73 \pm 0.75^{\text{ b}}$
1114	$22.36 \pm 0.43$ a	$3.79\pm0.51^{\circ}$	$14.31 \pm 0.23$ ab	$14.15 \pm 0.91  ^{\mathrm{ab}}$	$2.43 \pm 1.01^{\circ}$	$4.17\pm0.75\mathrm{bc}$	$5.88 \pm 0.75  \mathrm{bc}$
1130	$14.31 \pm 0.43$ a	$0.23 \pm 0.51^{\mathrm{b}}$	$11.36 \pm 0.23$ <sup>a</sup>	$1.92 \pm 0.91$ b	$0 \pm 0$	$2.59 \pm 0.75$ b	$313 \pm 0.75^{\mathrm{b}}$
1135	$21.01 \pm 0.43$ <sup>a</sup>	$0.32 \pm 0.51^{\mathrm{b}}$	$10.83\pm0.23\mathrm{ab}$	$0.92 \pm 0.91  ^{\mathrm{b}}$	$0 \pm 0$	$1.5 \pm 0.75$ b	$0.69 \pm 0.75^{\mathrm{b}}$
1140	$20.99 \pm 0.43$ a	$0.61\pm0.51^{\mathrm{b}}$	$10.20\pm0.23\mathrm{ab}$	$1.72 \pm 0.91$ b	$0 \pm 0$	$0.57 \pm 0.75^{\mathrm{b}}$	$0.14 \pm 0.75^{\mathrm{b}}$
1226	$29.48 \pm 0.43$ a	$10.40 \pm 0.51$ b	$16.69 \pm 0.23^{\mathrm{b}}$	$4.00\pm0.91^{\rm b}$	$4.43\pm1.01^{\mathrm{b}}$	$7.94 \pm 0.75^{\mathrm{b}}$	$11.75 \pm 0.75$

\*Mean  $\pm$  SD, Honey types: honeydew (Hd), polyfloral (Pf), rapesced (Bn), acacia (Rp), fruit trees (Pp), phacelia (Pt), clover (Tr), different letter mean significant differences (P < 0.05) between the columns.

The discriminant analysis technique was employed to evaluate the ability to distinguish between different honey types. A graphical representation of the FT-NIR and Raman spectral results is provided in Fig. 3 (Plate XI). Table 4 displays the correct classification rate (CCR) for the analysed honey samples, while Table 5 presents the confusion matrix for the cross-validation of results based on 20 randomized observations. The results demonstrate distinct differences between honeydew honey and monofloral honeys.

Table 4. Confusion matrix for the training data.

From\to	Rp	Tr	Pf	Hd	Pp	Pt	Bn	Total	CCR
Rp	7	0	0	0	0	0	0	7	100.00%
Tr	0	7	0	0	0	0	0	7	100.00%
Pf	0	0	94	0	0	0	0	94	100.00%
Hd	0	0	0	18	0	0	0	18	100.00%
Pp	0	0	0	0	5	0	0	5	100.00%
Pt	0	0	0	0	0	4	0	4	100.00%
Bn	0	0	1	0	0	0	25	26	96.15%
Total	7	7	95	18	5	4	25	161	99.38%

Honey types: honeydew (Hd), polyfloral (Pf), rapeseed (Bn), acacia (Rp), fruit trees (Pp), phacelia (Pt), clover (Tr) CCR – correct classification rate

Table 5. Confusion matrix for the cross-validation results.

From\to	Rp	Tr	Pf	Hd	Pp	Pt	Bn	Total	CCR
Rp	6	0	1	0	0	0	0	7	85.71%
Tr	0	7	0	0	0	0	0	7	100.00%
Pf	3	0	88	0	0	0	3	94	93.62%
Hd	0	0	0	18	0	0	0	18	100.00%
Pp	0	0	1	0	4	0	0	5	80.00%
Pt	0	0	0	0	0	4	0	4	100.00%
Bn	0	0	6	0	0	0	20	26	76.92%
Total	9	7	96	18	4	4	23	161	91.30%

Honey types: honeydew (Hd), polyfloral (Pf), rapeseed (Bn), acacia (Rp), fruit trees (Pp), phacelia (Pt), clover (Tr) CCR – correct classification rate

## Discussion

The peaks in the Raman spectra correspond to the content of each carbohydrate: glucose is characterized by values of 349, 844, and 1,226 cm<sup>-1</sup>; fructose corresponds to values of 553, 615, 695, 829 and 844 cm<sup>-1</sup>; sucrose is detected at 1,226 cm<sup>-1</sup> (Corvucci et al. 2015; Wu et al. 2022; Magdas and Berghian-Grosan 2023). The use of Raman spectra of the sugar profile proves to be a suitable complementary method for detecting the authenticity or botanical origin of honey, especially in combination with other methods and statistical techniques, as confirmed by Arvanitoyannis et al. (2005). In addition to the major carbohydrate content, the Raman spectrum also reflects the content of minor components such as pollen grains, minerals, proteins, waxes and other honey components (Manzanares et al. 2014). These minority components of honey can show the appearance of vibrational spectra near the peaks at wavenumbers 329, 349, 1,027, 1,135, 1,226 cm<sup>-1</sup> (Pierna et al. 2011).

Our measurement results indicate several statistically significant differences in individual vibrations (Table 1). The vibration in 308 cm<sup>-1</sup> is typical for glucose and has been assigned to a  $\delta(C-C-C)$  vibration and an endocyclic  $\delta(C-C-O)$  ring mode. For fructose, it originates from the  $\delta(C-C-C)$  ring vibration in the pyranoid form (Ozbalci et al. 2013). The vibration in 329 cm<sup>-1</sup> is associated with skeletal vibrational modes of C-C-C, C-C-O, and C-C bonds (Wu 2022). It occurs in glucose as a  $\delta$ (C-C-C) vibration and an endocyclic  $\delta(C-C-O)$  ring mode, and in fructose as originating from the  $\delta(C-C-C)$  ring vibration in the pyranoid and furanoid forms (Ozbalci et al. 2013). The vibration in 349 cm<sup>-1</sup> is attributed to an endocyclic  $\delta(C-C-O)$  ring mode of the glucose ring but also originates from the δ(C-C-C) ring vibration in the pyranoid and furanoid forms of the fructose ring (Ozbalci et al. 2013). The 543 cm<sup>-1</sup> vibration originates the α-glycosidic bond of C1 on the glucosyl subunit, and is also present in the maltose spectrum. It can be assigned to a C2-C1-O1 bending vibration in fluid honey. However, this band is absent in the Raman spectrum of crystallized honey, suggesting that it may depend on the water content (De Oliveira et al. 2002). The 562 cm<sup>-1</sup> vibration is assumed to the α-glycosidic bond of C1 on the glucosyl subunit, and is also observed in the sucrose spectrum (Ozbalci et al. 2013). Vibration in 602 and 606 cm<sup>-1</sup> corresponds to skeletal vibrations (Pierna et al. 2011). Vibration in 613 and 614 cm<sup>-1</sup> is assigned to the fructose spectrum (Ozbalci et al. 2013), vibration in 620 and 621 cm<sup>-1</sup> is attributed to ring deformations in fructose (Anjos et al. 2018; Aykas et al. 2020). They may be related to the bending of C-C-O, with exocyclic O involvement, given that there are 12 C-C-O angles, 10 of which are exocyclic (for both rings) (Mathlouthi and Luu 1980). The 695 cm<sup>-1</sup> vibration corresponds to the stretching of C-O and C-C-O bonds, as well as O-C-O bending. It is observed in the spectrum of sucrose and shows very weak intensity in D-glucose. It may be associated with the bending of C-C-O in the furanoid ring (Mathlouthi and Luu 1980; Anjos et al. 2018). Vibrations in 828 and 829 cm<sup>-1</sup> are linked to C-H and CH2 vibrations, as well as C-O-H bending in fructose. They likely arise from the v(C-C) vibration of fructopyranose and fructofuranose, respectively, with shifts due to the glycosidic bond with a glucose ring. They also involve  $\nu$ (C-C) and  $\delta$ (C1-H1) vibrations of  $\beta$ -glucose (Ozbalci et al. 2013; Aykas et al. 2020). The 844 cm<sup>-1</sup> vibration is assigned to the  $\nu$ (C-C) and  $\delta$ (C1-H1) vibrations of  $\alpha$ -glucose, and were widened and weakened in the maltose spectrum (Ozbalci et al. 2013). The 926 cm<sup>-1</sup> band may be assigned to the deformation of C-H out of the furanoid ring, but also this spectrum has been assigned to  $\delta$ (COH) and  $\nu$ (C-O) out-of-ring vibrations (Mathlouthi and Luu 1980; Ozbalci et al. 2013). Vibrations in 975 and 976 cm<sup>-1</sup> are assigned to the two anomers of fructose and glucose as v(C-O) vibration (Ozbalci et al. 2013; Anjos et al. 2018). Vibrations in 987, 990, 995, 997, and 999 cm<sup>-1</sup> are assigned to the deformation of C-H out of the pyranoid, and also to vibrations in the two anomers of fructose and glucose (Mathlouthi and Luu 1980; Anjos et al. 2018). Vibrations in 1,001 and 1,002 cm<sup>-1</sup> are assigned to C-6-H-2 (Mathlouthi and Luu 1980). Vibrations in 1,026 and  $1.028 \text{ cm}^{-1}$  are present in all honey spectra and can be assigned to a coupled v(C-C) and  $\nu$ (C-O) vibration of glucose and fructose. In the spectrum of glucose, these were assigned to the v(C-O) vibration in the two anomers pyranoid and furanoid rings, while the maltose and the sucrose spectra have been assigned to the v(C-O) vibration of the glucose ring (De Oliveira et al. 2002; Ozbalci et al. 2013). Vibration in 1,056 cm<sup>-1</sup> is assigned to the v(C-O) vibration in the pyranoid and furanoid rings, which could be C-C and C-O stretching modes of fructose (De Oliveira et al. 2002; Ozbalci et al. 2013). Vibrations in 1,111 and 1,114 cm<sup>-1</sup> are assigned to the  $\delta$ (C-O-C) angle-bending model (Ozbalci et al. 2013). Vibrations in 1,130, 1,135, and 1,140 cm<sup>-1</sup> are related to the C-OH deformation of glucose and sucrose, C-O-C cyclic alkyl ethers of fructose, CH and OH bending modes of glucose and sucrose, and the symmetric deformation mode of CH2 in fructose, respectively (Pierna et al. 2011; Aykas et al. 2020). The 1,226 cm<sup>-1</sup> vibration is associated

with the deformation vibration of C-C-H, O-C-H, and C-O-H in the vicinity (Pierna et al. 2011).

Table 3 shows the static differences in Raman spectra related to the composition. On the basis of specific vibrations, we are only able to distinguish certain honey types from each other. The exact classification has not been confirmed for any vibration. The consistency and differences in the wavenumbers are due to different compositions and amounts of carbohydrates and other substances contained. The most significantly different honeys were based on vibrations of 308, 606, 613, 620, 999 and 1,013 cm (Table 3) where there was a classification into 4 different groups (Pp, Pt, Hd, Bn) (P < 0.05). Our results are in agreement with the work of other authors, who also confirmed differences in the composition of single-species honeys and honeydew honeys, and thus differences in the specific wavenumbers measured by spectroscopic methods. In particular, these were wavenumbers characteristic of carbohydrates, specifically C-C-C and C-C-O vibrations and deformations (308, 606, 613, 620 cm<sup>-1</sup>) (Pierna et al. 2011; Ozbalci et al. 2013; Anjos et al. 2018). In addition, the wavenumbers 999 and 1,013 cm<sup>-1</sup>, which are typical of specific bioactive substances with pyran and furan rings (Ozbalci et al. 2013) and partially affected by fructose, glucose, maltose and sucrose anomers, were monitored. Pf honey showed the most frequent overlap with other honey types at these wavenumbers, with the most frequent matches being with rapeseed and acacia honeys. This result is expected, as rapeseed is the most common honey-producing plant in the Czech Republic. In acacia honey, due to the low pollen content, there is a relatively high presence of other pollen taxa that affect the bioactive content and thus the wavenumbers specific to pyran and furan rings (999 and 1,013 cm<sup>-1</sup>). For future research, greater emphasis should be placed on the sample sizes within the groups. Larger sample groups should be utilized to identify new and more specific signals from Raman and FT-NIR spectroscopy. The distinction between groups can also be achieved through domain decomposed classification algorithms for LDA analysis (Li and Cai 2024).

When honey is analysed using near-infrared spectroscopy (NIR), the NIR light interacts with the chemical components of the sample, creating a unique spectral fingerprint. This spectral fingerprint allows the identification of sugars, moisture, and organic compounds in honey (Cozzolino et al. 2011). The NIR calibration model is used to determine properties such as carbohydrate, moisture, protein and other components. Compared to traditional methods, NIR provides a rapid and non-invasive approach to honey analysis, allowing real-time measurements without compromising sample integrity (Ruoff et al. 2007). The use of the NIR method to detect honey adulteration was also used by Ruoff et al. (2006). Characteristic differences are noticeable at 4,200–7,100 cm<sup>-1</sup>. The largest variations in the spectra of individual honeys are noticeable in the 4,200-5,200 cm<sup>-1</sup> ranges (Ruoff et al. 2006). In our case, a significant difference between the different honey species is confirmed for the wavenumber 4,391 cm<sup>-1</sup>, where Bn, Pr, Tr, Pt form one group that is significantly different from other honey species (P < 0.05). Another significant spectrum is found at the wavenumbers 4,780 and 5,171 cm<sup>-1</sup>. Again, it is possible to distinguish between the different types of honeys; however, Rp, Tr, Pf, Bn and Pt honeys form one group that is significantly different from Pp and Hd honeys (P < 0.05). For the wavenumber 5,624 cm<sup>-1</sup> the split into two groups was confirmed, but only the Pp and Pf honeys are significantly different (P < 0.05).

Considering the large number of spectra analysed where some degree of differentiation of honey groups was confirmed in the Raman spectrum analysis, the data were processed using advanced statistical techniques similar to the work of Yong and Pearce (2013). Tests of higher statistical techniques allow a comprehensive evaluation of spectral curves obtained by both Raman spectroscopy and FT-NIR (Pataky et al. 2024). Ruoff et al. (2006) reported that the LDA method showed a correct classification rate between

39 and 63% for honey samples measured by Raman spectroscopy. The samples were mostly misclassified between polyfloral and rapeseed honey samples, whereas rapeseed honey samples were often classified as dandelion honeys, resulting in a correct classification in 63%. Ruoff et al. (2006) also stated that if only monofloral honey samples were selected for classification, the LDA could correctly classify more than 80% of the honey samples, with the exception of dandelion honey, which was correctly classified at 43% and rapeseed honey at 63%. The correct classification among monofloral honeys was 85% (Ruoff et al. 2006). Our measured results confirmed the higher CCR, which was 100% for Pp, Hd, Pf, Tr, Rp, Pt. In agreement with (Ruoff et al. 2006), our results confirmed a lower CCR for rapeseed honey, which was 96.15% (Table 4). For validation, the model was further cross-validated where the average CCR was 91.3% (Table 5). The model also achieved a high classification rate for Hd, Pt and Tr honey samples, where the classification accuracy was 100%; while 93.62% was achieved for Pf honey, 85.71% for Rp honey and 80% for Pp honey. The lowest CCR was for the Bn honey, namely 76.92%, which is similar to the training samples for LDA.

By analysing the spectra using FT-NIR and Raman spectroscopy by LDA, we achieved a higher CCR of 99.38% in our study with cross-validation, compared to 91.3% than using Raman spectroscopy alone, which achieved 63% (Ruoff et al. 2006).

Several key conclusions can be drawn from the results of this work. Combinations of Raman spectroscopy and FT-NIR spectroscopy are proving to be highly effective tools for determining the botanical origin of honey. The selected model showed a high reliability, exceeding 95%, for honeydew honey samples as well as monofloral honey samples of phacelia and clover. In contrast, for other types of honey, including polyfloral honey samples, the model is less reliable and its application would require the analysis of a larger sample group of various honey samples to construct a more valid model. Most of the analysed FT-NIR spectra revealed significant differences in the intensity of the measured wavenumbers, which contributes in a major way to a more accurate classification of the different honey species. On the other hand, Raman spectroscopy identified a broader range of specific wavenumbers relevant to honey classification and provided insights into components beyond carbohydrates, including bioactive substances associated with characteristic vibrations of pyranoid and furanoid rings. The combination of the two methods resulted in a better classification performance than that commonly reported in the literature for single applications of Raman spectroscopy and FT-NIR spectroscopy. Although precise identification of individual components requires further confirmation using techniques such as HPLC or GC-MS, FTIR can be considered a suitable screening tool for preliminary compositional comparison of plant extracts. Future research could focus on validating these results through multi-method approaches and on expanding the range of analysed samples, including possible quantification of selected functional groups based on spectral features.

## Acknowledgements

The study was supported by the Applied Research Programme of the Ministry of Agriculture for the 2017-2025 period [Project No. QK1920344, 'ZEMĚ' ('The Land')].

## References

Ahmed AS, Sulaiman SA, Baig AA, Ibrahim M, Liaqat S, Fatima S, Jabeen S, Shamim N, Othman NH 2018: Honey as a potential natural antioxidant medicine: an insight into its molecular mechanisms of action. Oxid Med Cell Longev 2018: 1-19

Anjos O, Santos AJA, Paixao V, Estevinho LM 2018: Physicochemical characterization of *Lavandula* spp. honey with FT-Raman spectroscopy. Talanta 178: 43-48

Arvanitoyannis IS, Chalhoub C, Gotsiou P, Lydakis-Simantiris N, Kefalas P 2005: Novel quality control methods in conjunction with chemometrics (multivariate analysis) for detecting honey authenticity. Crit Rev Food Sci Nutr 45: 193-203

- Aykas DP, Shotts ML, Rodriguez-Saona LE 2020: Authentication of commercial honeys based on Raman fingerprinting and pattern recognition analysis. Food Control 117: 107346
- Bogdanov S, Jurendic T, Sieber R, Gallmann P 2008: Honey for nutrition and health: a review. J Am Coll Nutr 27: 677-689
- Cianciosi D, Forbes-Hernández TY, Gasparrini SAM, Redo-Rodriguez P, Manna PP, Zhang J, Lamas LB, Florez SM, Toyos PA, Quiles JL, Giampieri F, Battino M 2018: Phenolic compounds in honey and their associated health benefits: a review. Molecules 23: 2322
- Combarros-Fuertes P, Fresno JM, Estevinho MM, Sousa-Pimenta M, Tornadijo ME, Estevinho LM 2020: Honey: Another alternative in the fight against antibiotic-resistant bacteria? Antibiotics 9: 1-21
- Corvucci F, Nobili L, Melucci D, Grillenzoni FV 2015: The discrimination of honey origin using melissopalynology and Raman spectroscopy techniques coupled with multivariate analysis. Food Chem 169: 487-494
- Cozzolino D, Corbella É, Smyth HE 2011: Quality control of honey using infrared spectroscopy: a review. Appl Spectrosc Rev 46: 523-538
- De Oliveira LFC, Colombara R, Edwards HGM 2002: Fourier transform Raman spectroscopy of honey. Appl Spectrosc 56: 306-311
- El Sohaimy SA, Masry SHD, Shehata MG 2015: Physicochemical characteristics of honey from different origins. Ann Agric Sci 60: 279-287
- García NL, Amadei Enghelmayer M 2025: The complexity of honey fraud detection. Bee World 102: 8-14
- Jerković I, Kuś PM 2014: Terpenes in honey: Occurrence, origin and their role as chemical biomarkers. RSC Adv 4: 31710-31728
- Li J, Cai XC 2024: Domain decomposed classification algorithms based on linear discriminant analysis: An optimality theory and applications. Neurocomputing **575**: 127261
- Magdas DA, Berghian-Grosan C 2023: Botanical honey recognition and quantitative mixture detection based on Raman spectroscopy and machine learning. Acta A Mol Biomol Spectrosc 293: 122433
- Mandal MD, Mandal S 2011: Honey: its medicinal property and antibacterial activity. Asian Pac J Trop Biomed 1: 154-160
- Manzanares AB, Garcia ZH, Galdon BR, Rodriguez ER, Romero CD 2014: Physicochemical characteristics of minor monofloral honeys from Tenerife, Spain. LWT Food Sci Technol 55: 572-578
- Mathlouthi M, Luu DV 1980: Laser-Raman spectra of d-fructose in aqueous solution. Carbohydr Res **78**: 225-233 Ozbalci B, Boyaci IH, Topcu A, Kadilar C, Tamer U 2013: Rapid analysis of sugars in honey by processing Raman spectrum using chemometric methods and artificial neural networks. Food Chem **136**: 1444-1452
- Pataky J, Demalis EC, Shelly J, Miller K, Moore ZM, Vidt ME 2024: Use of a factor analysis to assess biomechanical factors of American Sign Language in native and non-native signers. J Biomech 165: 112011
- Pierna JAF, Abbas O, Dardenne P, Baeten V 2011: Discrimination of Corsican honey by FT-Raman spectroscopy and chemometrics. Biotechnol Agron Soc Environ 15: 75-84
- Rodriguez-Saona LE, Fry FS, McLaughlin MA, Calvey EM 2001: Rapid analysis of sugars in fruit juices by FT-NIR spectroscopy. Carbohydr Res 336: 63-74
- Ruoff K, Luginbühl W, Bogdanov S, Bosset JO, Estermann B, Ziolko T, Amado R 2006: Authentication of the botanical origin of honey by near-infrared spectroscopy. J Agric Food Chem 54: 6867-6872
- Ruoff K, Luginbühl W, Bogdanov S, Bosset JO, Estermann B, Ziolko T, Kheradmandan S, Amado R 2007: Quantitative determination of physical and chemical measurands in honey by near-infrared spectrometry. Eur Food Res Technol 225: 415-423
- Samarghandian S, Farkhondeh T, Samini F 2017: Honey and health: a review of recent clinical research. Pharmacogn Res 9: 121-127
- Smith BC 2011: Fundamentals of Fourier Transform Infrared Spectroscopy. 2nd edn. Boca Raton: CRC Press, 207 p.
- Tsagkaris AS, Koulis GA, Danezis GP, Martakos I, Dasenaki M, Georgiou CA, Thomaidis NS 2021: Honey authenticity: analytical techniques, state of the art and challenges. RSC Adv 11: 11273-11294
- Wu X, Xu B, Ma R, Gao S, Niu Y, Zhang X, Du Z, Liu H, Zhang Y 2022: Botanical origin identification and adulteration quantification of honey based on Raman spectroscopy combined with convolutional neural network. Vib Spectrosc 123: 103439
- Yong AG, Pearce S 2013: A beginner's guide to factor analysis: focusing on exploratory factor analysis. Tutor Quant Methods Psychol 9: 79-94

# Plate X Pleva B. et al.: Raman ... pp. 251-259 Variables (axes F1 and F2: 59.25)

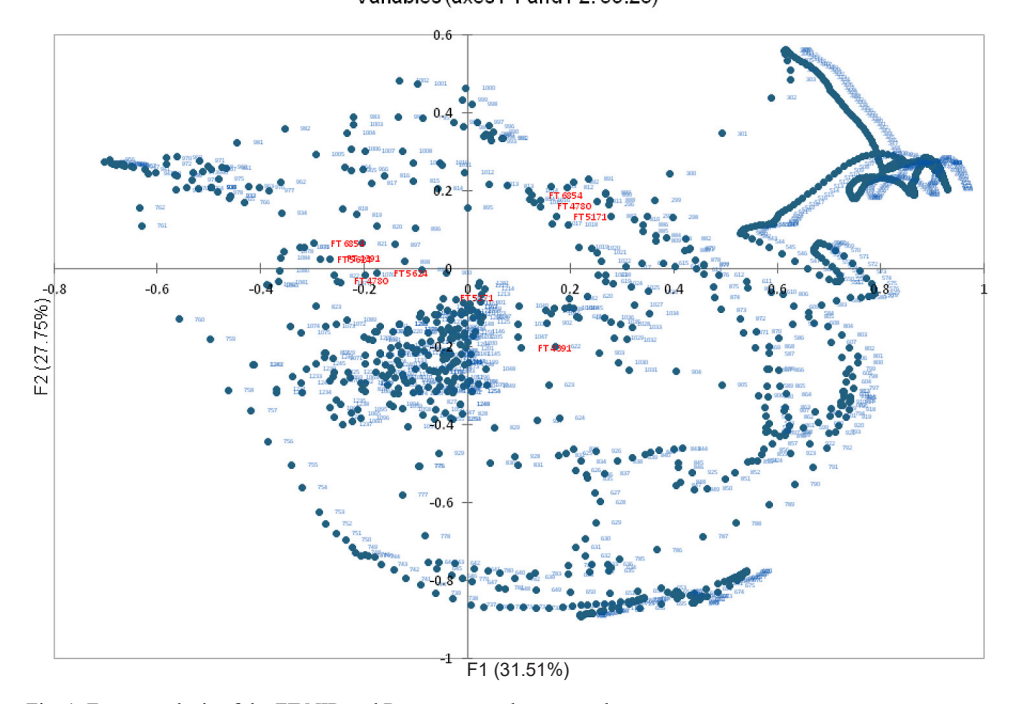


Fig. 1. Factor analysis of the FT-NIR and Raman spectral wavenumbers. Individual wavenumbers: Red FT-NIR, blue Raman

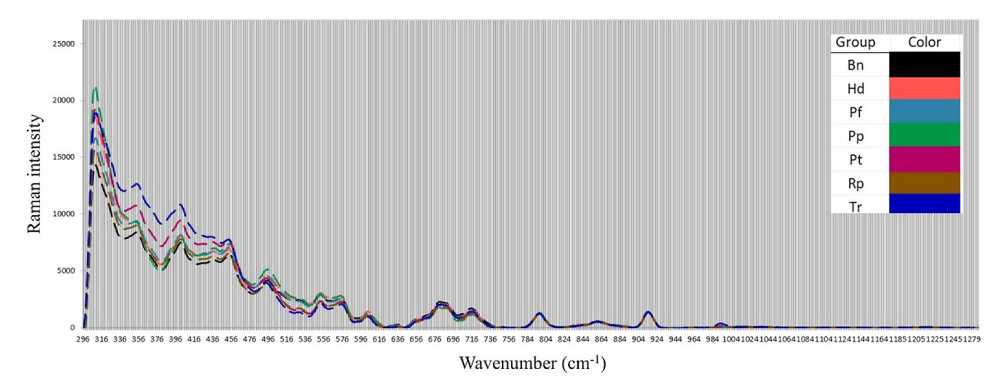


Fig. 2. Raman spectra of honey types in region between 200 cm<sup>-1</sup> and 1,280 cm<sup>-1</sup>. Honeydew (Hd), polyfloral (Pf), rapeseed (Bn), acacia (Rp), fruit trees (Pp), phacelia (Pt), clover (Tr)

# Observations (axes F1 and F2: 59.25%)

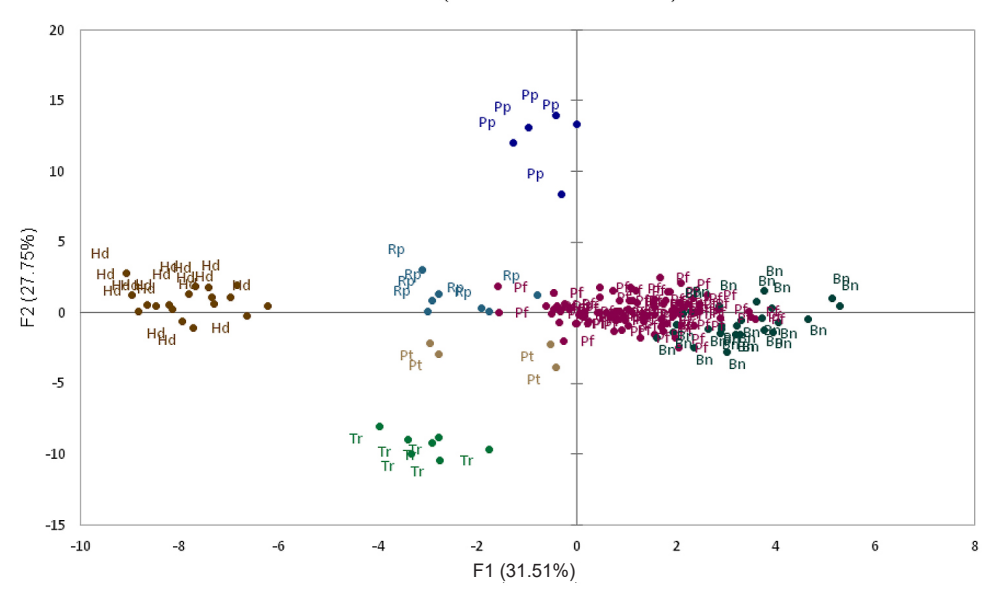


Fig. 3. Linear discriminant analysis of FT-NIR and Raman spectra. Honeydew (Hd), polyfloral (Pf), rapeseed (Bn), acacia (Rp), fruit trees (Pp), phacelia (Pt), clover (Tr)